ELSEVIER

Journal of Wind Engineering
and Industrial Aerodynamics 96 (2008) 1152–1163

JOURNAL OF wind engineering AND industrial aerodynamics

www.elsevier.com/locate/jweia

Investigation of bluff body asymmetry on the properties of vortex shedding

Adriana L. Csiba[a], Robert. J. Martinuzzi[b,*]

[a]*Department of Mechanical and Materials Engineering, The University of Western Ontario, London, Ont., Canada N6A 5B9*

[b]*Department Mechanical and Manufacturing Engineering, University of Calgary, Calgary, Alta., Canada T2N 1N4*

Available online 3 August 2007

Abstract

The influence of unequal strength opposing shear layers on periodically shed vortices is experimentally investigated in the wake of a two-dimensional triangular cylinder. The experiment was developed to isolate the influence of the intensity differential between two shear layers from other flow parameters. Phase-averaged velocity and surface pressure data were obtained for a Reynolds number of 22 500. The relative intensity of the shear layers was adjusted through the angle of incidence. It is found that the shedding frequency can be satisfactorily scaled using the projected obstacle width. The product of the drag and shedding frequency scales with the velocity parameter k, based on the base pressure, as predicted from existing theory. However, the predicted relationship between k and the shedding frequency no longer holds, indicating that the existing vortex shedding theory needs modification to account for unequal strength shear layers.

Keywords: Bluff body wakes; Vortex shedding; Asymmetry; Phase-averaging; Vortex strength

1. Introduction

The periodic shedding of vortices from high aspect ratio bluff bodies gives rise to important periodic lateral loading and is a major contribution to the mean drag. Vortex shedding is associated with the vibration of transmission wires and the aerodynamic instability of suspension bridges or tall chimneys. The intensity of the shed vortices is also

*Corresponding author. Tel.: +1 403 220 6627; fax: +1 403 282 8406.
E-mail address: rmartinu@ucalgary.ca (R.J. Martinuzzi).

0167-6105/$ - see front matter © 2007 Published by Elsevier Ltd.
doi:10.1016/j.jweia.2007.06.037

Nomenclature

a	streamwise vortex spacing
b	transverse vortex spacing
C_D	drag coefficient
C_p	pressure coefficient
C_{pb}	base pressure coefficient
D	cylinder side length
D'	projected cylinder side length
f_s	shedding frequency
k	base pressure parameter
P	pressure
Re	Reynolds number
St_D	Strouhal number based on the D of the cylinder
$St_{D'}$	Strouhal number based on the projected D' of the cylinder
U	streamwise component of velocity
U_c	convective speed of vortices
U_s	velocity on free streamline at separation
U_∞	freestream velocity
x	streamwise direction in laboratory coordinate system
y	transverse direction in laboratory coordinate system

Greek symbols

α	angle of incidence
ρ	fluid density
γ	circulation of a shed vortex
Γ_0	initial circulation generated at the separation point

important for the dispersion of scalar fields. Consequently, the prediction of the oscillation frequency, the force magnitude and wake dynamics is an important concern for structural and environmental engineering. While most fundamental studies focus on flows with an inherent symmetry, it can be argued that most practical applications involve varying degrees of asymmetry due to an angle of incidence relative to the mean flow.

The formation of the Kármán vortex street (von Kármán, 1912) for two-dimensional symmetric bluff bodies has been comprehensively discussed (cf. Gerrard, 1966; Bearman, 1967). Opposite sign circulation, generated at the flow separation points on the opposite faces of the obstacle, gives rise to equal intensity, but opposing sign shear layers in the wake. The coupled instabilities of these shear layers result in the formation of two staggered rows of regularly spaced, counter-rotating vortices of equal intensity moving at the same convective speed. Existing models (Roshko, 1954; Bearman, 1967) rely extensively on this inherent symmetry for predicting the shedding frequency, the induced drag and relating base pressure to the strength of the shed vortices.

The structure of the Kármán vortex street is characterized by the convective speed of the vortices, U_c, their circulation, γ, and the streamwise-to-transverse vortex spacing

ratio, b/a. von Kármán (1912) showed that for two parallel rows of vortices of equal but opposing circulation a stable arrangement of vortices exists only if $b/a = 0.281$, which implies a universal Strouhal number since the streamwise spacing is the product of the convective speed and shedding frequency. Several studies (cf. Fage and Johansen, 1927; Bearman, 1967; Cantwell and Coles, 1983; Lyn et al., 1995) have shown that b/a is obstacle-geometry dependent. However, Roshko (1954) showed that it was possible to define a wake Strouhal number, which was constant for several obstacle geometries. Instead of using U_c, the velocity scale is chosen as that of the free streamline at the separation points, U_s, and the length scale as the distance between the free streamlines. With this approach, U_s can be related directly to the base pressure and the average circulation generated at the separation point and thus a direct estimates of b/a becomes unnecessary.

Roshko's universal wake Strouhal number has been shown to be sensitive to the free stream turbulence level and its usefulness is considered doubtful (Gerrard, 1966; Bearman, 1967; Lee, 1975). Bearman (1967) proposed to use U_s and the transverse vortex spacing, b, as scales. This approach also yields a unique relationship between U_s and the product of the drag and shedding frequency. Lee (1975) showed that both this new Strouhal number and the drag–velocity relationships hold over a larger range of turbulence levels and obstacle geometries.

The above formulations rely extensively on the inherent symmetry of the opposing shear layers and it is still not well understood how the strength of the shed vortices and their downstream structure are modified when the opposing shear layers are of unequal strength. In this work, the influence of unequal strength shear layers on the structure of the shed vortex street is investigated experimentally. A triangular prism is used at different angles of incidence. Surface pressure and phase-averaged velocity data are compared to predictions based on existing theory.

2. Experimental techniques

The experiments were performed in an open suction-type wind tunnel with an inlet contraction ratio of 4:1. A hexagonal mesh flow straightener and three fine-wire meshes were located at the inlet. The working section was 2.1 m long with a 460 mm × 460 mm cross-section. The obstacle was placed at the centre of the working section. The approach flow velocity, U_∞, was uniform within 0.5% across the working section, except for the wind tunnel wall boundary layers (approximately 20 mm thick). The turbulence intensity of the approach flow was approximately 1%.

The obstacle, a smooth surface, acrylic triangular cylinder of 21 mm × 21 mm × 30 mm cross-section, spanned the entire working section (460 mm), resulting in an aspect ratio of 15.33 based on $D = 30$ mm. The assembly and nomenclature are shown in Fig. 1. The coordinate system (x, y) origin was located at the centreline of the base (leeward) cylinder face. Tests were conducted for U_∞ ranging from 5 to 15 m/s, corresponding to Re of 10 000–30 000 based on U_∞ and D.

Simultaneous surface pressure measurements were made at 13 pressure taps (diameter of 0.8 mm), of which nine were located along the cylinder centreline as shown in Fig. 1a. Four pressure taps were located along the cylinder leading face at the level of Tap P2 at $z = \pm 2.2D$ and $\pm 5D$ to verify the mean flow two-dimensionality. The effective blockage due to the cylinder was approximately 6.9%. All pressure data presented are thus

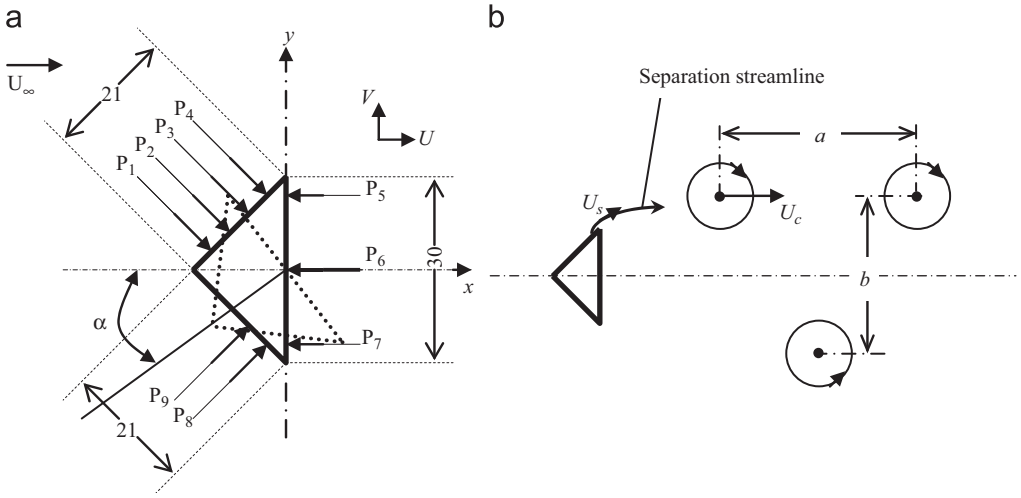

Fig. 1. Nomenclature and schematic representation of (a) the cylinder geometry showing the pressure tap locations. Dimensions are given in mm. Taps P1–P4 are distributed 5 mm apart with Tap P4 at 2 mm from the trailing edge. Taps P9 and P8 are located across Taps P3 and P4, respectively. Taps P5 and P7 are located on the leeward side at 2 mm from the trailing edge and P6 is located at the centre. (b) Parameters used to describe the structure of the vortex street.

blockage-corrected following West and Apelt (1981). The pressure data acquisition system comprised two 16-channel scanning pressure transducers (Pressure Systems Inc. Model ESP-16). Pressure data were acquired simultaneously from the pressure taps and Pitot-static tube (for U_∞). Pressure results are reported as pressure coefficients:

$$C_p = \frac{P - P_\infty}{\frac{1}{2}\rho U_\infty^2},$$

where the reference static pressure and velocity (P_∞ and U_∞) were determined from a barocell in parallel and were also were used to automatically calibrate the pressure transducers at the beginning of each acquisition. The differential pressure transducer had a range of 0–250 Pa and a resolution of ± 0.5 Pa. An initial calibration of the pressure system (tubing, taps, transducer), using a loudspeaker, showed that the pressure signals were undamped for frequencies below 200 Hz. The pressure taps were simultaneously sampled at 400, 500 and 650 Hz for 60 s (or at least 1200 shedding cycles). The shedding frequency, f_s, was estimated directly from the power spectra.

Velocity measurements for $\alpha = 0^\circ$ and 10° were made with a two-component laser Doppler velocimeter (LDV) in backscatter mode using a 4 W Ar-ion laser light source. A 2.6× beam expander and 480 mm focal length lens with a beam spacing of 130 mm resulted in a measuring volume diameter of 46 μm and a length of 340 μm. Atomized oil provided light-scattering particles of 2 μm number mean diameter. Velocity data were processed using an IFA 650 processor (TSI Inc.) with a coincidence window of 400 μs after determining that the velocity cross-correlation coefficient was independent of the coincidence window between 50 and 500 μs. The LDV probe was positioned by a three-axis traverse of accuracy at ± 1 mm/1 m travel.

To determine the wake vortex structure and circulation, a phase-averaging technique was used. The velocity field is represented using the double-decomposition:

$$U_i(t) = \langle U_i \rangle + u_i',$$

where $U_i(t)$ is the measured velocity component, $\langle U_i \rangle$ is the phase-averaged (coherent) and u_i' is the incoherent contribution to the velocity component. Pressure signals from taps located at the upper (P4) and the lower (P8) trailing edges provided the phase reference to synchronize the velocity field. Only one reference signal is necessary for synchronization. If the coherent and incoherent estimates calculated using the two reference signals varied by more than the calculated uncertainty, the measurement point was rejected. Each cycle was then mapped on 20 equal width phase bins. When compared to distributions using 40 phase bins, the results were within experimental uncertainty.

The uncertainty analysis was conducted following Coleman and Steele (1999) based on the ANSI/ASME (1986) standard. The uncertainty on the shedding frequency was ± 0.2 Hz (0.4%), on the instantaneous pressure measurement, $C_p(t)$, ± 0.05 and on the mean pressure, C_p, ± 0.02. The uncertainty for the mean and coherent components of velocity are $\pm 0.01 U_\infty$ and $\pm 0.04 U_\infty$, respectively, and $\pm 10\%$ for the circulation.

3. Results

3.1. Influence of the angle of incidence on the Strouhal number

Experiments were conducted for angles of incidence $\alpha = 0^\circ$, 10°, 20° and 30°, for $10\,000 \leqslant Re \leqslant 30\,000$. The mean pressure distributions on the obstacle faces were obtained at the locations shown in Fig. 1a and are presented as mean pressure coefficients, C_p. The C_p-distribution for $\alpha = 0^\circ$, shown for different Re in Fig. 2, is symmetric about $y = 0$ and is constant on the leeward face. Results for this case and other α show that the Re-influence

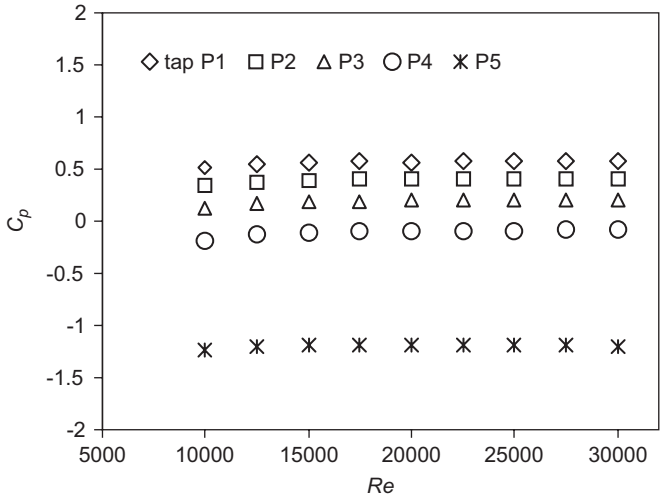

Fig. 2. Distribution of the mean pressure coefficient, C_p, as a function of Reynolds number for $\alpha = 0^\circ$. For tap location, refer to Fig. 1.

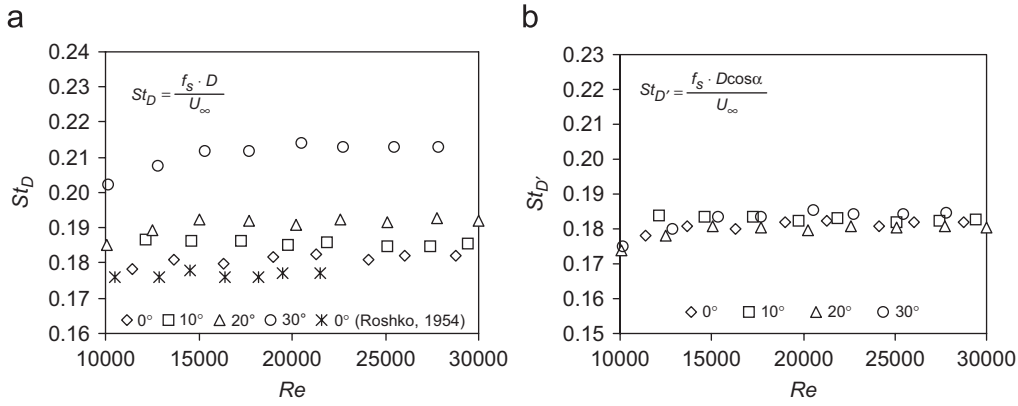

Fig. 3. Blockage corrected (a) Strouhal number St_D and (b) modified Strouhal number $St_{D'}$ as a function of the Reynolds number, Re, for different angles of incidence, α.

on the C_p-distribution is negligible in this range and can be represented by the results for $Re = 22\,500$.

Blockage corrected Strouhal numbers, $St_D = f_s D/U_\infty$, are shown in Fig. 3a as a function of Re for different angles of incidence. The results of Roshko (1954) for a triangular cylinder at $\alpha = 0^\circ$ are also shown and found to agree within experimental uncertainty. For $Re > 13\,000$, the influence of the Re on St_D can be considered negligible. However, for smaller Re, there is a slight influence for $\alpha = 20^\circ$ and 30°. The reason for this effect is unclear. Redefining the Strouhal number based on the projected width, $D' = D\cos\alpha$, leads to a collapse of all $St_{D'}$-data onto a single curve within experimental uncertainty as shown in Fig. 3b. Assuming that the separation of the shear layers in the wake will be proportional to D', these results suggest that a Strouhal number based on the wake parameters would have more general validity as indicated by Roshko (1954) and Bearman (1967).

Fig. 4 compares the influence of the incidence angle, α, on the shedding frequency for different sharp-edged cylinders. When based on D, the Strouhal number, St_D, generally increases with α. When using $D' = D\cos\alpha$ as a length scale, $St_{D'}$ is independent of α, albeit for each geometry the value of the constant is different.[1] Assuming that the shear layers separate at the trailing edge without interfering with the after-body, changing α should result in a change in the relative shear layer intensity (strength) ratio without modifying the vortex formation region (Luo et al., 1994). These results then support the analysis of Bailey et al. (2003), which predicts that the vortex spacing ratio is unaffected by the relative strength of the shear layers. However, as shown in Table 1, the spacing ratio appears to depend on the obstacle geometry.

3.2. Base pressure and velocity scale

von Kármán's early work suggests the existence of a universal Strouhal number, S_K, since the streamwise vortex spacing, $a = U_c/f_s$, where f_s is the shedding frequency and U_c is

[1]For the square cylinder in the range $35^\circ < \alpha \leqslant 45^\circ$ the after-body interferes with the shear layers and thus the behaviour is modified.

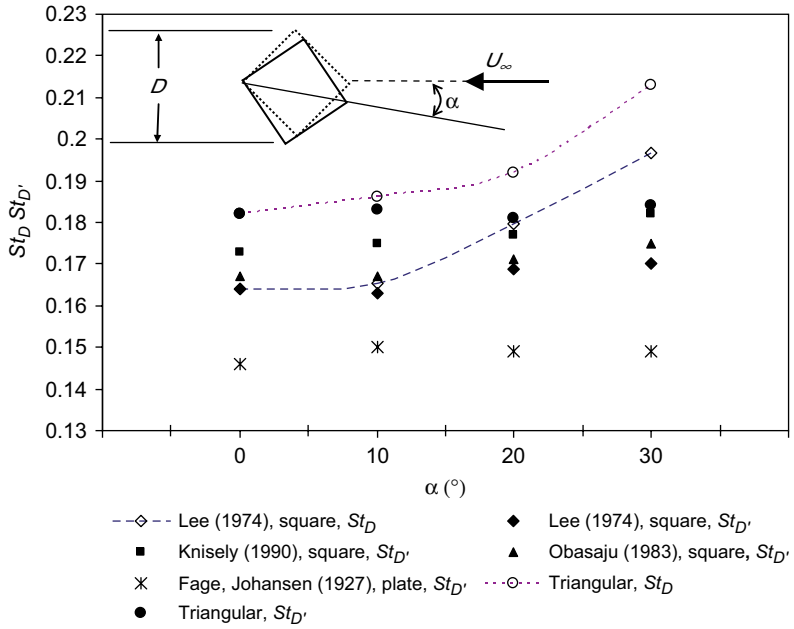

Fig. 4. Comparison of St_D and $St_{D'}$ of triangular cylinder with different shapes of bluff bodies at $\alpha = 0°$, 10°, 20° and 30°. D refers to the diagonal dimension (Lee, 1974; Knisely, 1990; Fage and Johansen, 1927; Obasaju, 1983).

Table 1
Comparison of spacing ratios and initial circulation

Source	Geometry	b/a	$\Gamma_0/U_\infty D$	γ/Γ_0
von Kármán (1912)	Theory	0.28		
Present work	Triangle, $\alpha = 0°$	0.22	6.1	0.42
	Triangle, $\alpha = 10°$	0.25	6.0	0.47
Lyn et al (1995)	Square, $\alpha = 0°$	0.19	10	0.45
Cantwell and Coles (1983)	Circular, $\alpha = 0°$	0.16	5.9	0.44
Luo et al. (1994)	Triangle, $\alpha = 180°$	0.21	3.0	
	Triangle, $\alpha = 190°$	0.20	3.1	

the vortex convective speed, such that

$$\frac{b}{a} = \frac{bf_s}{U_c} = \text{constant}.$$

Early observations (cf. Fage and Johansen, 1927) that b/a depends on the obstacle geometry have led to modifications of S_K. Roshko (1954) suggested

$$S_K = \frac{f_s h'}{U_s} = \frac{f_s h}{U_\infty}\frac{U_\infty}{U_s}\frac{h'}{h} = St\frac{1}{k}\frac{h'}{h},$$

where h is the obstacle width, h' is the shear layer separation and U_s is the velocity on the streamline at the point of separation given in terms of the base pressure, C_{pb}, by

$$k = \frac{U_s}{U_\infty} = \sqrt{1 - C_{pb}}.$$

Lee (1975) noted that S_K is influenced by the freestream turbulence and suggested that the definition of Bearman (1967) is preferable:

$$S_B = St\frac{1}{k}\frac{b}{h}.$$

Bearman (1967) suggests a value of $S_B \approx 0.181$ and Lee (1975) reported that for a wide range conditions, data for flows around circular and square cylinders, the value of S_B ranges from 0.172 to 0.187. In the present experiments, $St_{D'} = St_D \cos\alpha = 0.182 \pm 0.002$, implying that

$$\frac{b}{h} = \frac{S_B}{St}k \approx k\ \cos\ \alpha.$$

The question can thus be formulated: does the concept of the universal Strouhal number extend to cases where the opposing shear layers are of different strength?

Fig. 5 shows the mean pressure distribution, C_p, at the trailing edge of the windward faces, the back pressure, C_{pb}, and the drag coefficient, C_D, as functions of the angle of incidence, α. As α increases, C_p increases along the upper face and decreases along the lower face, which is consistent with the expectation that the velocities will differ at the trailing separation as asymmetry increases. This observation implies that intensity of the opposing shear layers (and, thus, the circulation shed) will differ. However, C_{pb} remains surprisingly uniform along the leeward face.

Bearman (1967) also showed that the product of the drag coefficient and the Strouhal number, $C_D St$, is uniquely related to k. In Fig. 6, $C_D St_D$ is shown as a function of k for square and triangular cylinders for different α. The data of Bailey (2001), labelled 45°(τ),

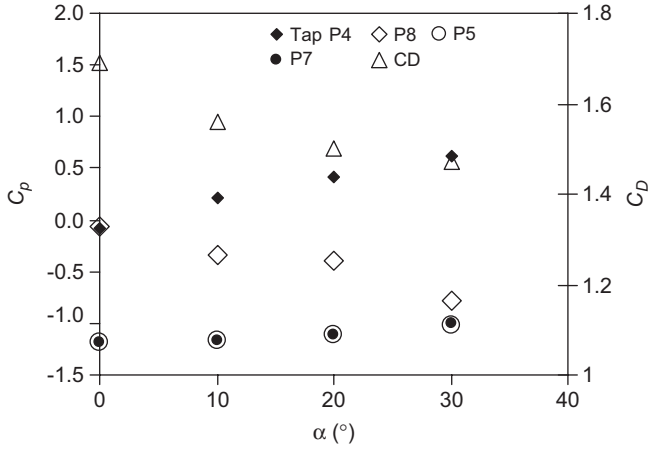

Fig. 5. Pressure distribution, C_p, and drag coefficient, C_D, as a function of the angle of incidence, α. Tap P4, Tap P8—upper and lower windward face upstream of trailing edge; Tap P5, Tap P7, C_{pb}—leeward face near trailing edge.

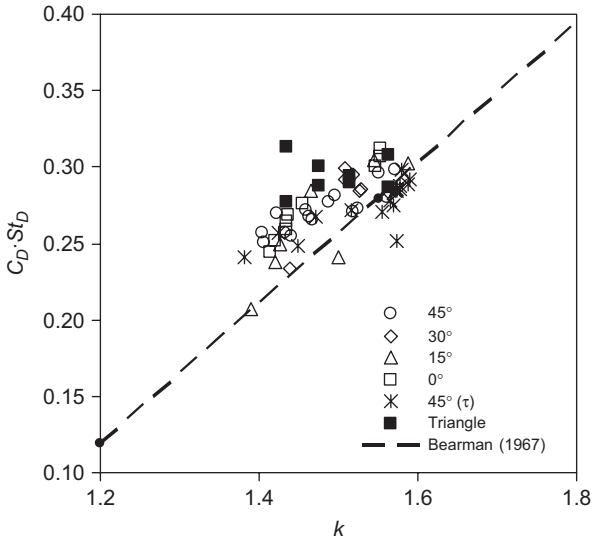

Fig. 6. Product of drag coefficient and Strouhal number, $C_D St_D$, as a function of the speed parameter k for square and triangular prisms for different angles of incidence. Square prism data from Bailey et al. (2003) and Lee (1975). Data 45°(τ) represents data for square cylinder with one face normal to flow and different on-coming shear conditions (Bailey, 2001). Broken line represents predicted values by Bearman (1967) using Kronauer minimum drag criterion as per Lee (1975).

represent the case of a square cylinder with one face normal to the flow ($\alpha = 45^\circ$) at different distances from a solid wall and thus express the influence of an on-coming shear flow. The agreement between these data and the predictions of Bearman (1967) (broken line) is surprisingly good. In the original derivation, k is related to the pressure directly behind the separation point, which is assumed to be the same as C_{pb}, assuming equal intensity opposing shear layers. For the triangle and square cylinder at $\alpha > 20^\circ$ all of these conditions generally do not hold, although C_{pb} is uniform on the leeward face for all cases.

3.3. Investigation of the vortex street

Analysis of the velocity field in the wake of the triangular cylinder for $\alpha = 0^\circ$ and 10° provides additional insight into the shedding process for unequal intensity shear layers. In Fig. 7, the mean streamwise velocity components at $x/D = 0$ and 1.6 are compared. These locations correspond to the trailing edge (leeward face) and the approximate end of the recirculation region, respectively. At $x/D = 0$, the asymmetry of the two shear layers for $\alpha = 10^\circ$ is evident. Due to the intense mixing in the base region, however, these differences are rapidly mitigated downstream as seen at $x/D = 1.6$. The recirculation region for $\alpha = 10^\circ$ is slightly longer than for $\alpha = 0^\circ$ and the maximum velocity deficit is located slightly off-centre indicating that the wake is slightly skewed.

The circulation of the shed vortices, γ, and their convective velocity, U_c, can be estimated from the coherent velocity field obtained from the phase-averaged measurements. The vortex cores were identified using the pressure field second invariant criterion of Jeong and Hussain (1994), the centroid of the vortices were associated with the peaks of the second

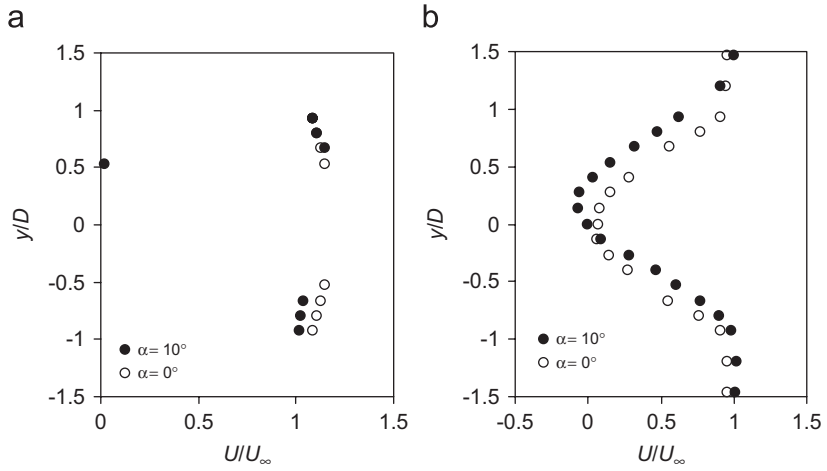

Fig. 7. Mean streamwise velocity component (normalized by U_∞) for $\alpha = 0^\circ$ and 10° at (a) $x/D = 0$ and (b) $x/D = 1.6$.

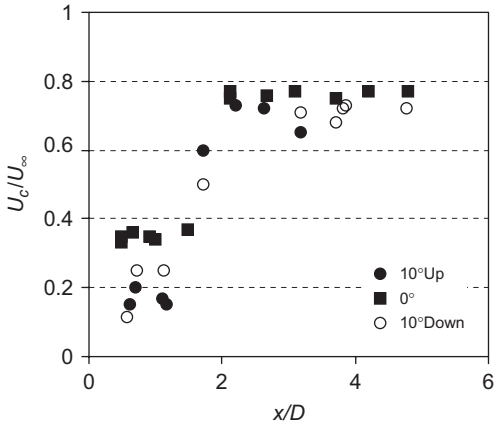

Fig. 8. Convective velocity, U_c/U_∞, for $\alpha = 0^\circ$ and 10° as a function of x/D.

invariant and the motion of the peaks was used to estimate the average U_c shown in Fig. 8. Similarly to the results of Cantwell and Coles (1983) and Lyn et al. (1995), the shed vortices move slowly in the formation region. The end of the formation region can be recognized by the rapid increase of the convective velocity. Further downstream, U_c is constant for both shear layers, approximately $0.76U_\infty$ and $0.72U_\infty$ for $\alpha = 0^\circ$ and 10°, respectively. The streamline topology for the shed vortices is viewed in the reference frame moving at the downstream convective speed. For example in Fig. 9 for $\alpha = 10^\circ$, the core and the associated saddle point for the downstream vortex can be clearly identified. Note that for the base vortices, which move at a different U_c, the streamline topology is distorted and not representative.

The circulation shed from each vortex is obtained using $\gamma = \int \vec{\Omega} \cdot d\vec{A}$, where Ω is the vorticity and A is the vortex core area defined by the closed streamline originating at the

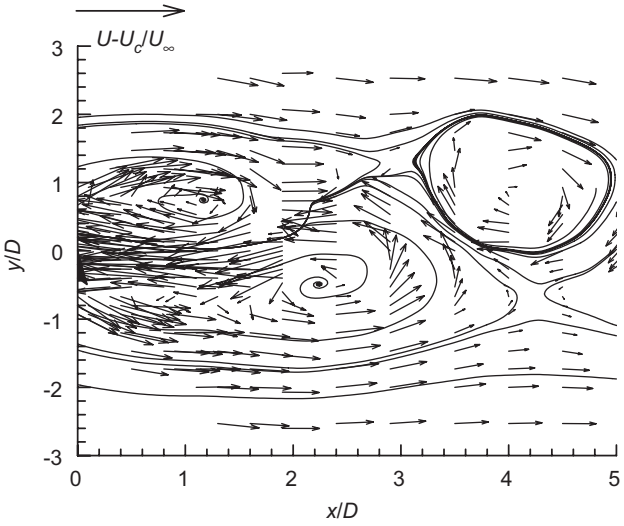

Fig. 9. Sample phase-averaged velocity field for arbitrary phase of the shedding cycle in the reference frame $U_c/U_\infty = 0.72$ for $\alpha = 10^\circ$.

saddle point. The average circulation is shown in Table 1, where the initial circulation is, according to Roshko (1954):

$$\frac{\Gamma_0}{U_\infty D} = \frac{1 - C_{pb}}{2St} = \frac{k^2}{2St}.$$

The data obtained for different bluff body shapes shows that while the initial circulation can change widely, the ratio γ/Γ_0 is very similar and around 0.45. The circulation associated with the mean shear layer can be estimated at the trailing edge of the obstacle from:

$$\frac{\Gamma}{U_\infty D} = \frac{1}{2St}(U_2^2 - U_1^2),$$

where the subscripts 1 and 2 correspond to the minimum and maximum streamwise components above and below the shear layer. Thus, it is expected that $\gamma/\Gamma_0 = 1 - \Gamma/\Gamma_0$. Using the data from Fig. 7a, for $\alpha = 0^\circ$ yields $\Gamma/\Gamma_0 \approx 0.6$ or $\gamma/\Gamma_0 \approx 0.4$, which is close to the estimate of 0.42 given in Table 1. For $\alpha = 10^\circ$, $\Gamma/\Gamma_0 \approx 0.59$ and 0.51 for the top and bottom shear layers. Using the average value of 0.55 yields an average value of $\gamma/\Gamma_0 \approx 0.45$, which is again very close to the value of 0.47 calculated from the velocity data. Thus, the relationship relating k, C_{pb} and Γ_0 holds in an average sense.

4. Conclusions

The flow over a two-dimensional triangular cylinder was experimentally investigated using pressure measurements and phase-averaged LDV. Tests were conducted at several angles of incidence to generate unequal intensity opposing shear layers. It is found that the modified Strouhal number, based on the projected width of the obstacle, was independent of the angle of incidence. The existence of vortex shedding for unequal shear

layers is consistent with the description of Bailey et al. (2003). The velocity parameter k (Roshko, 1954), relating base pressure, C_{pb}, to the initial circulation, Γ_0, is a valid "average" representation of the influence of the two unequal shear layer strengths and represents well the product of drag and shedding frequency as predicted by Bearman (1967). However, the latter's definition of the universal Strouhal number does not provide a reliable prediction of the vortex spacing. Specifically, while the theory predicts that b/a decreases according to $k\cos\alpha$, these experiments suggest that the vortex spacing ratio actually increases with α. These results suggest that the classical theory based on equal strength shear layers only partially captures the behaviour for shedding with unequal shear layers and requires further modification.

References

Bailey, S.C.C., 2001. Wall proximity effect on square cylinder vortex shedding. M.Sc. Thesis. University of Western Ontario, London, Canada.

Bailey, S.C.C., Kopp, G.A., Martinuzzi, R.J., 2003. The vortex shedding from the square cylinder close to a solid wall. J. Turbul. 3, 1–18.

Bearman, P.W., 1967. On vortex street wakes. J. Fluid Mech. 28, 625–641.

Cantwell, B., Coles, D., 1983. An experimental study of entrainment and transport in the turbulent near wake of a circular cylinder. J. Fluid Mech. 136, 321–374.

Coleman, B.J., Steele Jr., W.G., 1999. Experimentation and Uncertainty Analysis for Engineers, second ed. Wiley, New York.

Fage, A., Johansen, F.C., 1927. The Structure of Vortex Sheets, R.&M. No. 1143, British A.R.C.

Gerrard, J.H., 1966. The mechanics of the formation region of vortices behind bluff bodies. J. Fluid Mech. 25 (2), 401–413.

Jeong, J., Hussain, F., 1994. On the idenfication of a vortex. J. Fluid Mech. 285, 69–94.

Knisely, C.W., 1990. Strouhal numbers of rectangular cylinders at incidence: a review and new data. J. Fluids Struct. 4, 371–393.

Lee, B.E., 1975. The effect of turbulence on the surface pressure field of a square prism. J. Fluid Mech. 69 (2), 263–282.

Luo, S.C., Yazdani, M.G., Chew, Y.T., Lee, T.S., 1994. Effects of incidence and afterbody shape on flow past bluff cylinders. J. Wind Eng. Ind. Aerodyn. 53, 375–399.

Lyn, D.A., Einav, S., Rodi, W., Park, J.-H., 1995. A laser-Doppler velocimetry study of ensemble-averaged characteristics of the turbulent near wake of a square cylinder. J. Fluid Mech. 304, 285–319.

Obasaju, E.D., 1983. An investigation of the effects of incidence on the flow around a square section cylinder. Aeronaut. Q. 34, 243–259.

Roshko, A., 1954. On the drag and shedding frequency of 2-D bluff bodies, NACA. Technical Note 3/69.

von Kármán, T., 1912. Uber den Mechanismus des Wiederstandes, den ein bewegter Korper in einer Flussigkeit erfaehrt.m Gottingen Nachr., Math-Phys. Klasse, pp. 547–556.

West, G.S., Apelt, C.J., 1981. The effects of tunnel blockage and aspect ratio on the mean flow past a circular cylinder with Reynolds numbers between 10^4 and 10^5. J. Fluid Mech. 114, 361–377.